Decoupled illumination detection in light sheet microscopy for 4D observation of spermatozoa at high-resolutions

Jacob Licea-Rodriguez[1,2*], *Gustavo* Castro-Olvera[2], *Omar* Palillero-Sandoval[1], *Gonzalo* Merino[3,4], *Martin* Eriksen[3,4], *Roberto* Beltrán-Vargas[1], *Israel* Rocha-Mendoza[5], *Omar E.* Olarte[6] and *Pablo* Loza-Alvarez[2*]

[1]Centro de Investigación en Ingeniería y Ciencias Aplicadas, Universidad Autónoma del Estado de Morelos, Ave. Universidad 1001, Cuernavaca 62209, México
[2]ICFO–Institut de Ciències Fotòniques, The Barcelona Institute of Science and Technology, Castelldefels 08860, Spain
[3]Institut de Física d'Altes Energies (IFAE), The Barcelona Institute of Science and Technology, Campus UAB, 08193 Bellaterra (Barcelona), Spain
[4]Port d'Informació Científica (PIC), Campus UAB, C. Albareda s/n, 08193 Bellaterra (Barcelona), Spain
[5]Centro de Investigación Científica y de Educación Superior de Ensenada, Carretera Ensenada-Tijuana, No. 3918, Zona Playitas, 22860 Ensenada B. C., México
[6]Department of Physics, Universidad Nacional de Colombia, 111321, Bogotá, Colombia

Abstract. We present the use of wavefront coding (WFC) combined with machine learning in a light sheet fluorescence microscopy (LSFM) system. We visualize the 3D dynamics of sperm flagellar motion at an imaging speed up to 80 volumes per second, which is faster than twice volumetric video rate. By using the WFC technique we achieve to extend the depth of field of the collection objective with high numerical aperture (NA=1) from 2.6 µm to 50 µm, i. e., more than one order of magnitude. To improve the quality of the final images, we applied a machine learning-based algorithm to the acquired sperm raw images and to the point spread function (PSF) of the generated cubic phase masks previous to the deconvolution process.

1 Introduction

Structural details and motility of spermatozoa are essential criteria for assessing sperm health and viability. Motility is also important from the perspectives of fundamental biology and in general in reproductive health problems [1,2]. Spermatozoa exhibit several kinds of motility modes and swimming patterns during their natural 3D motion. Particularly, imaging the sperm flagellum dynamics is of great interest to assess the health and viability of the sperm. However, due to the flagellum's small diameter and rapid oscillating pattern, visualizing it with sufficient time and spatial resolution presents a challenge. To address this, a fast volumetric and high resolution imaging technique is indispensable. Light sheet fluorescence microscopy (LSFM) has been used in the past to record the fast 3D processes that occur in a large number of applications, including the fields of neuroscience and developmental cell biology [3,4]. A useful strategy for fast volumetric imaging is achieved by combining LSFM with wavefront coding (WFC). In this case, the depth-of-field (DoF) of the collection objective can be extended and, importantly, the light sheet can be axially scanned within this extended DoF [5]. By doing so, the sample remains static and volumetric imaging speeds of up to 75 volumes/s have been recorded. In this way, the image acquisition speed will only be limited by the reading speed of the camera. Due to the short integration times, images are often modulated by a reduced signal to noise ratio. On the other hand, machine learning has recently been used in biological imaging to enhance the quality of biomedical images. Specifically, the denoising of images attempts to remove instrumental noise. In this work, we present the use of WFC combined with machine learning (specifically, applying the noise2void algorithm [6]) in a LSFM system under high numerical aperture (NA) conditions. This system has allowed us to visualize the 3D dynamics of sperm flagellar motion at an imaging speed up to 80 volumes/s, which is faster than twice volumetric video rate.

2 LSFM + WFC setup

The general scheme of the optical setup of LSFM+WFC is shown in Fig. 1. Briefly, the light sheet at 488 nm is generated in the xy-plane by a galvanometric mirror (not shown) and projected on the sample. The fluorescence generated in the illuminated plane is collected by the water immersion objective, CO (20x, NA=1, Olympus), placed orthogonal to the light sheet. This collection arm contains a deformable mirror (DM) lying in a conjugated plane with the exit pupil of the collection objective. This, by the use of a cubic phase mask, results in an extension of the DoF. A Shack-Hartmann wavefront sensor WFS, located in an auxiliary path and also in a configuration of conjugated planes with the DM, is used to ensure that the correct phase is added to the DM. Finally, the

* Corresponding author: jacob.licea@uaem.mx, pablo.loza@icfo.eu

fluorescence signal passing by DM is collected by the CMOS camera.

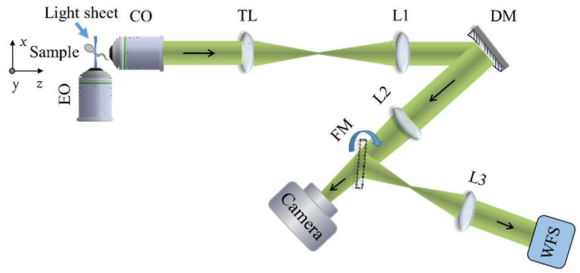

Fig. 1. General scheme of the LSFM+WFC system setup. In the scheme: EO: excitation objective; CO: collection objective; TL: tube lens; L: lens; DM: deformable mirror; FM: flip mirror; WFS: wavefront sensor

3 Results

3.1 Phase mask characterization

The phase mask used in WFC produces an elongated axial PSF that gives rise to the extension of the DoF. Due to the use of the phase mask, the acquired images are distorted. The images are restored by using a digital deconvolution method based on the measured PSF. Figs. 2a and 2b show the experimental three-dimensional PSF along the z axis for the flat phase mask (FPM) and cubic phase mask (CPM). In this example, the DoF of the collection objective is extended from 2.6 µm to more than 50 µm (more than one order of magnitude larger).

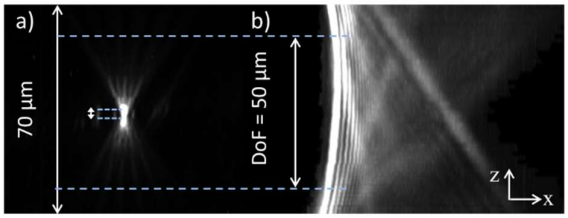

Fig. 2. a) Experimental three-dimensional PSF along the z axis for the phase masks. a) FPM and b) CPM

3.2 free swimming pork sperm imaging

The acquired raw images are distorted and noisy. Previous to the deconvolution process, we applied the denoising noise2void algorithm based on machine learning to remove instrumental noise of the acquired images. The deconvolved and denoised images of a free swimming sperm corresponding at a single plane for a visualization speed of 80 volumes/s are shown in Fig. 3. The visualized image volume contains 5 planes resulting in a volume depth of 40 µm. The imaging speed achieved is faster than twice the volumetric video rate, which allows capturing the beating oscillatory behavior in 3D of the flagellar movement of the spermatozoa. The traces of intensity versus time of the region indicated with the inset square is also presented. As it can be seen, it is possible to observe a sperm flagellar beat frequency of ~22 Hz.

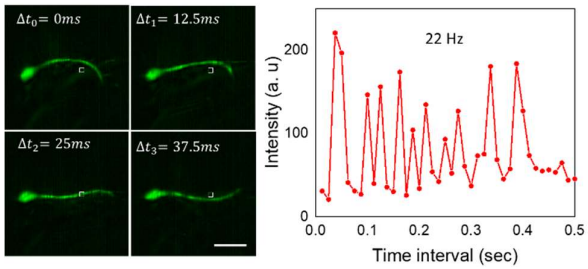

Fig. 3. Deconvolved and denoised images of a single plane at different time intervals for an imaging speed of 80 vol/s. Intensity profile of the inset square considering a time interval of 0.5 s. Scale bar: 20 µm

4 Conclusions

We have implemented the technique of WFC combined with machine learning in a LSFM system to perform fast volumetric high resolution imaging. With this technique, we have extended the depth of field of a high numerical aperture objective lens more than one order of magnitude. In a LSFM configuration, this allows quickly moving the light sheet through the sample to visualize the full observed volume without having to move the sample. Furthermore, the image contrast and signal-to-noise ratio was improved using the denosing (noise2void) algorithm based on machine learning. The capability of fast volumetric imaging of our LSFM-WFC system was demonstrated by visualizing the 3D sperm flagellar motion at an imaging speed up to 80 volumes/s, which is faster than twice volumetric video rate imaging. Imaging the full beating of the sperm flagellum in 3D with high temporal and spatial resolutions gives a strong indication of the sperm motility and health. This may have important implications for fundamental fertility studies in biology, food industry and in reproductive health problems.

References

1. C. C. Lim, S. E. M. Lewis, M. Kennedy, E. T. Donnelly, W. Thompson, Andrologia **30,** 43-47 (1988)
2. P. Fernández-López, J. Garriga, I. Casas, M. Yeste, F. Bartumeus, Commun. Biol **5**, 1027 (2022)
3. Y. Wan, K. McDole, P. J. Keller, Annu. Rev. Cell Dev. Biol **35**, 655-681 (2019)
4. O. E. Olarte, J. Andilla, E. J. Gualda, P. Loza-Alvarez, AOP **10**, 111-179 (2018)
5. O. E. Olarte, J. Andilla, D. Artigas, P. Loza-Alvarez, Optica **2**, 702-705 (2015)
6. A. Krull, T. O. Buchholz, F. Jug, *Proceedings on the IEEE/CVE Conference*, 2129-2137 (2019)